

Rapidly rotating stars with either H burning or He burning core

M. Shindo¹, M. Hashimoto¹, Y. Eriguchi², and E. Müller³

¹ Department of Physics, Kyushu University, Ropponmatsu, Fukuoka 810, Japan

² Department of Earth Science and Astronomy, University of Tokyo, Komaba, Tokyo 153, Japan

³ Max-Planck-Institut für Astrophysik Karl-Schwarzschild-Str.1, D-85740, Garching, Germany

Received 18 December 1996 / Accepted 28 March 1997

Abstract. We have succeeded in constructing structures of realistic models for rapidly rotating inhomogeneous stars in the nuclear burning stages. The nuclear reaction networks both for CNO cycle and for helium burning have been successfully included in the 2D numerical code. Concerning the equation of state and the opacity, we have used the same ones as used in calculations of spherical stellar structures. The rotation law in our computations covers uniform rotation and differential rotation with rapidly rotating cores. We have computed several equilibrium sequences of massive stars up to models just before the mass begins to shed from the equatorial surface (critical models).

We mainly discuss two critical sequences of models: 1) $18 M_{\odot}$ stars with hydrogen burning cores and 2) $5 M_{\odot}$ helium stars with helium burning cores. It is found that the effect of rotation on the structure is similar for both sequences. For uniformly rotating hydrogen burning stars the luminosity decrease is about 6.4% which is consistent with the results obtained by other authors. For models which have the angular momentum distribution concentrated toward the center, we get very flattened shapes of stellar surfaces. Compared with the non-rotating models, decrease of the luminosity is found to be 16% for the critical models if the total angular momentum is less than $10^{53} \text{ g cm}^2 \text{ s}^{-1}$ and if a toroid-like structure of the density distribution does not appear. On the other hand, decrease of the luminosity becomes significant for stars with the toroid-like structure of the density distribution, i.e. for *toroidal* distribution of the energy source. It is remarkable that stars whose ratio of the polar radius to the equatorial radius is less than 0.25 have extended envelopes due to a delicate balance between the gravitational force and the centrifugal force.

Key words: nuclear reactions– accretion – stars:rotation

1. Introduction

In the last several decades a considerable progress has been achieved in understanding the stellar evolution. For spherical

Send offprint requests to: M. Hashimoto

symmetric stars, we can calculate stellar evolutions starting from the zero-age main-sequence stars (e.g. Maeder & Meynet 1987, 1988) and ending to the pre-supernova progenitors (Nomoto & Hashimoto 1988). These calculations are considered to be *realistic* because the most updated physics which is essential to determine the stellar structure is included: the opacity, the equation of state, the nuclear reaction, the weak interaction and other physical processes. As a consequence, the theory of stellar evolution is regarded as the most successful field in astrophysics (see e.g. Kippenhahn & Weigert 1990). In particular, it has been proved that the one-dimensional (or spherical symmetric) code of stellar evolution has been remarkably useful to explain astrophysically important phenomena such as SN1987A (see e.g. Saio et al. 1988).

However, from the observational point of view, there have been many observations of rotating stars as well as spherical stars. For example, projected rotational velocities of some O-Type stars are observed to exceed 400 km s^{-1} (Penny 1996). Observations of supernovae such as SN1987A (Papaliolis et al. 1989) and SN1993J (Trammell et al. 1993) suggest asymmetries of explosions which might be related to rotation of stellar cores. Nevertheless the effect of rotation on the various stages of stellar evolution is still very uncertain. The current status of stellar models which include rotation is discussed by Pinsonneault (1996).

Therefore we need to investigate *realistic* rotating stars from the theoretical standpoint. Although there have been many investigations about *realistic* rotating stars (e.g. Roxburgh et al. 1965; Faulkner et al. 1968; Jackson 1970; Kippenhahn & Thomas 1970; Sackmann 1970; Sackmann & Anand 1970; Bodenheimer 1971; Whelan et al. 1971; Papaloizou & Whelan 1973; Clement 1978, 1979, 1994), rotation has been taken into account through perturbation methods by assuming *slow* rotation, except for the works by Jackson (1970), Bodenheimer (1971) and Clement (1978, 1979, 1994). Those results of slow rotation approximation show how the luminosity and the radius change. For uniformly rotating massive main-sequence stars, decrease of the luminosity is about $6 \sim 8\%$ and decrease of the polar radius is about $1 \sim 3\%$. In particular, Whelan et al. (1971) found that the polytropic approximation for realistic

stars such as main-sequence stars gives poor results concerning the luminosity.

For *rapidly rotating* realistic stars, the first reliable and quantitative investigation was the work by Bodenheimer (1971). He examined the effect of angular momentum on upper-main-sequence stars of 15, 30 and 60 M_{\odot} . He included all the necessary physical processes available at that time into his two-dimensional calculations and discussed how rapid rotation changed the structure of the star. He found a substantial effect on the mass-luminosity relation for differentially rotating models with large total angular momenta. It should be noted that his models did never reach the stages of mass shedding except for uniformly rotating stars. This is partly because his method which was based on the self-consistent-field (SCF) method developed by Ostriker & Mark (1968) could not give solutions for highly deformed configurations. After his pioneer study, Clement (1979, 1994) has solved equilibrium structures of rapidly rotating realistic stars based on the newly developed difference scheme. In his papers he obtained equilibrium sequences of differentially rotating main sequence stars of 1, 1.5, 3, 5, 10 and 15 M_{\odot} . However, his code could not give converged solutions for models of polytropes with $K/|W| > 0.26$ where K and W are the rotational energy and the gravitational energy, respectively (Clement 1974) and for models of realistic stars with $K/|W| > 0.14$ (Clement 1978, 1979, 1994). Clement argued that those two critical values correspond to the stability limits for the secular and dynamical bar mode instabilities. Nevertheless it seems strange that he could not obtain converged solutions for models with larger values of $K/|W|$ because his scheme is based on the Newton's method which is likely to give *even* unstable solutions (see e.g. Eriguchi and Müller 1985). Although dynamically unstable configurations need not be solved, we had better get solutions which may suffer from secular instabilities, i.e. models with $0.14 < K/|W| < 0.26$. Moreover input physics used by Bodenheimer (1971) and Clement (1979, 1994) is too simplified compared with that used in spherical stellar evolutions. Therefore, it is necessary to clarify the effect of very rapid rotation on the stellar structure by taking more detailed physical processes into account and by using more powerful numerical schemes than those of Bodenheimer (1971) and Clement (1978, 1979, 1994).

When we try to solve rapidly rotating stars, we encounter serious problems to overcome. Even if we restrict ourselves to axisymmetric or two-dimensional problems, it is very difficult to perform a reliable stellar evolutionary calculation. One main reason is the difficulty in handling self-gravity of stars with the realistic physical processes if stars deform considerably. Although the SCF method used by Bodenheimer (1971) and the difference scheme developed by Clement (1978, 1979) are schemes to handle real stars, they could not be applied to highly deformed stars as mentioned before, even if barotropic equations of state such as polytropes are employed.

In such a situation Eriguchi & Müller (1985) developed a new numerical code to get equilibrium structures of considerably deformed polytropes with any polytropic indexes (see also the references referred to in Eriguchi et al. 1986). There-

fore there arises a possibility that we will be able to investigate significantly deformed *realistic* stars. In fact Eriguchi & Müller (1991, 1993) have succeeded for the first time in developing a powerful scheme to construct rapidly rotating equilibrium configurations of very deformed stars with simplified equations of state and with nuclear burning approximated by an explicit formula (e.g. Clayton 1968). However, their physical inputs are too simple to explore the effect of rotation on the realistic structure.

In the present paper, we will extend their scheme to more realistic stellar models. In other words, we include the realistic physics which is crucial to determine the stellar properties: the opacity, the equation of state and the nuclear energy generation. Then we construct rotating stellar models as realistically as possible and investigate the effect of rotation on the structure of stars.

In Sect. 2 we explain basic assumptions of our approach, the input physics and the numerical scheme. Initial models are given in Sect. 3. Results are presented in Sect. 4. In Sect. 5 discussions and concluding remarks are given.

2. Assumptions and numerical methods

Basic assumptions and basic equations are almost the same as those used in Eriguchi & Müller (1991) except input physics. Thus we will briefly summarize the assumptions, the equations and the numerical schemes as well as a new treatment of input physics.

2.1. Assumptions

We assume the stars to be stationary, axisymmetric and inviscid. We allow chemical compositions X_i to be inhomogeneous. Note that X_i stands for all types of nuclei we take into account.

Although in realistic rotating stars there will arise meridional circulations in the radiative region, we assume that the circulation velocity is so small that only first order terms with respect to the circulation velocity will be taken into account. In other words circulations do not appear in the equation of motion. The only circulation velocity to be taken into account is that in the energy equation. Since we are interested in the global or averaged internal structures of rotating realistic stars, we will not need to calculate the circulation field. As is shown later, the velocity term can be eliminated by averaging the energy equation on the constant temperature surfaces. Thus we will not refer to the distribution of the circulation field in this paper.

Concerning the rotation law, although there can be a route to solve the rotation law by assuming that circulation fields will not arise within the radiative region (see e.g. Tassoul 1978; Uryu & Eriguchi 1994, 1995), we will not choose this standpoint. If we allow circulation fields to excite, we need to specify the rotation law because an inviscid fluid is assumed. In principle we can choose any kind of rotation law as far as it satisfies stability conditions (see e.g. Tassoul 1978). For simplicity we will assume the angular velocity Ω depends only on the distance

from the rotational axis:

$$\Omega = \Omega(r \sin \theta) , \quad (1)$$

where the spherical coordinates (r, θ, φ) are used. Under the assumptions mentioned above, this rotation law implies the stars to be pseudo-barotrope; i.e. the constant surfaces of the density, the temperature, the pressure, the composition, and the total potential coincide each other. Since configurations are pseudo-barotropic, we can choose the temperature as a basic variable. In other words, once this choice is made, it is enough to specify the central temperature to solve the internal structures.

2.2. Input physics

Concerning the equation of state, we include contributions of the electron, the ion and the radiation; the total pressure $P(\rho, T, X_i)$ can be expressed by the sum of the electron pressure P_e , the ion pressure P_{ion} and the radiation pressure P_{rad} as follows:

$$P = P_e + P_{ion} + P_{rad} . \quad (2)$$

Here P_e includes the electron-degeneracy and P_{ion} includes the Coulomb effect (Nomoto & Hashimoto 1988) and ρ and T are the density and the temperature, respectively.

As for the nuclear energy generation rate $\varepsilon_n(\rho, T, X_i)$, we include hydrogen burning (CNO-cycle) and helium burning that are important for the early stage of evolution of massive stars. The network for the CNO cycle (CNO-network) contains 12 nuclear species: ^1H , ^4He , ^{12}C , ^{13}C , ^{13}N , ^{14}N , ^{15}N , ^{14}O , ^{15}O , ^{16}O , ^{17}O , ^{17}F . This network has been constructed by using the scheme devised by Müller (1986). The energy generation rate, the composition change, and the temperature change are calculated simultaneously from the nuclear reaction network code. Furthermore, to simulate helium burning, we have used the α -network (Müller 1986) which contains 13 nuclear species: ^4He , ^{12}C , ^{16}O , ^{20}Ne , ^{24}Mg , ^{28}Si , ^{32}S , ^{36}Ar , ^{40}Ca , ^{44}Ti , ^{48}Cr , ^{52}Fe , ^{56}Ni .

We have included the realistic opacity which consists of the appropriate formulae of Stellingwert (1975) in the temperature range $T < 10^7\text{K}$ and of Iben (1975) in the range of $T > 10^7\text{K}$ (see also Saio et al. 1988).

2.3. Basic equations and boundary conditions

Under the assumptions discussed before, the hydrostatic equation can be expressed as

$$\frac{1}{\rho} \nabla P = -\nabla \phi_g + r \sin \theta \Omega^2 \mathbf{e}_R , \quad (3)$$

where ϕ_g and \mathbf{e}_R are the gravitational potential and the unit vector in the R direction, respectively. Here $R = r \sin \theta$. It should be noted that circulation velocities are neglected. The gravitational potential satisfies Poisson's equation:

$$\Delta \phi_g = 4\pi G \rho . \quad (4)$$

The energy equation for the star with the circulation velocity \mathbf{u} in the radiative region can be expressed as

$$\rho T \mathbf{u} \cdot \nabla s = \rho \varepsilon_n - \nabla \cdot \mathbf{F} , \quad (5)$$

where the quantities s and ε_n are the specific entropy and the energy generation rate, respectively. The energy flux \mathbf{F} is defined by

$$\mathbf{F} = -\frac{4acT^3}{3\kappa\rho} \nabla T . \quad (6)$$

Here a , c and $\kappa(\rho, T, X_i)$ are the radiation constant, the speed of light and the opacity per unit mass, respectively.

As for the boundary conditions, the physical quantities are regular all through the space and the surface is defined by a set of points where the pressure vanishes:

$$P = 0 . \quad (\text{on the surface}) \quad (7)$$

Concerning the gravitational potential, it is regular everywhere and tends to zero at infinity:

$$\phi_g \rightarrow 0 . \quad (r \rightarrow \infty) \quad (8)$$

In our numerical scheme, instead of using Poisson's equation (4) directly, we will use the following integral form for the gravitational potential because we can easily take the boundary condition (8) into account and avoid troubles related to the free boundary value problem (see e.g. Eriguchi and Müller 1984):

$$\phi(\mathbf{r}) = -G \int \frac{\rho d^3 \mathbf{r}'}{|\mathbf{r} - \mathbf{r}'|} . \quad (9)$$

2.4. Equations in the temperature space

Since configurations are pseudo-barotropic, i.e. most physical quantities can be regarded as functions of the temperature alone, we will devise to express the energy equation by considering the temperature as one of the *independent* variables.

First of all it should be noted that because of the stationarity of the structure, the flux of the matter must not cross the temperature constant surface. Therefore Eq. (5) can be integrated to the following form:

$$\int_V (\rho \varepsilon_n - \nabla \mathbf{F}) = 0 , \quad (10)$$

where V is the volume between two constant temperature surfaces. By making use of the equation of motion and noting that configurations are pseudo-barotropic, this Eq. (10) can be expressed as follows:

$$\frac{d \ln P}{d \ln T} = -\frac{4acT^4}{3\kappa P} \frac{\int_{S_T} \nabla P / \rho d\mathbf{S}}{\int_V \rho \varepsilon_n dV} , \quad (11)$$

where S_T denotes the surface of the volume V on which the temperature is constant. For a spherically symmetric star, this equation is reduced to that of radiative equilibrium.

In the convective region we will use the adiabatic pressure-temperature relation:

$$\frac{d \ln P}{d \ln T} = \left(\frac{\partial \ln P}{\partial \ln T} \right)_s . \quad (12)$$

For the criterion of convection, we have adopted the Schwarzschild criterion as has been done for the spherical evolution calculations. Therefore, the distribution of compositions inside the convective region is assumed to be uniform.

2.5. Rotation law

As discussed before, since we do not know the real angular momentum distribution inside the star, we must assume the rotational law. In the present investigation, we have examined the following rotation law which covers two extreme cases: the uniform rotation law and the case where the specific angular momentum j is asymptotically constant in space:

$$\Omega = \frac{\Omega_0}{1 + (R/B)^2} . \quad (13)$$

Here Ω_0 and B are the angular velocity on the rotation axis and a rotation parameter which characterizes the degree of differential rotation. For a large value of B , the relation (13) approaches to the law of uniform rotation. For a small value of B , the specific angular momentum j approaches constant for most part of the stars. From the point of stellar evolution, it might be reasonable to assume that rotation is uniform after the angular momentum redistribution during evolution. However, there exist neither observational data nor reliable theories for the rotation laws inside the star. Thus we had better investigate possibilities that the stellar core may rotate differentially and rapidly. Validity of the choice of the relation (13) has been discussed in detail by Eriguchi et al. (1986). For the convective regions it might be usual to assume uniform rotation. However in this investigation, we will use the rotation law (13) throughout the whole star.

2.6. Numerical scheme

The numerical scheme is almost the same as that used by Eriguchi & Müller (1991, 1993). We will describe only the essential parts of the numerical scheme here.

We note that the equation of motion (3) can be integrated to the following form:

$$\int \frac{dP}{\rho} = -\phi_g + \phi_{\text{rot}} + C , \quad (14)$$

where C is an integration constant and ϕ_{rot} is the rotational potential defined by

$$\phi_{\text{rot}} \equiv \int R \Omega^2 dR . \quad (15)$$

It should be noted that the left hand side of Eq. (14) is the enthalpy H , i.e.

$$H \equiv \int \frac{dP}{\rho} . \quad (16)$$

In order to solve equations, we use two different spaces, i.e. the ordinary coordinate space (r, θ, φ) and the temperature space where the temperature is treated as the independent variable as mentioned before. In the coordinate space we calculate the gravitational potential and the rotational potential. By applying the boundary conditions, we can determine the value of the integral constant. From these two potentials and the integral constant, we can calculate the value of the enthalpy at every point in the coordinate space.

Since the enthalpy is the thermodynamical quantity, it can be expressed as a function of the temperature in our situation because of pseudo-barotropy. In other words the enthalpy can be calculated from the thermodynamical structure which is obtained by integrating Eq. (11) or (12) in the *temperature space*. Therefore we can have two expressions for the enthalpy, one in the coordinate space and the other in the temperature space. By equating these two expressions we can obtain the temperature distribution in the coordinate space. This in turn enables us to have distributions of other quantities such as the density, the pressure and so on in the coordinate space. The obtained structure can be used to compute new values of the gravitational and the rotational potentials. In this way equations can be iteratively solved.

In actual computations we have used mesh numbers $(r \times \theta) = (101 \times 41)$ in the coordinate space, and 600 points in the temperature space. Typically a converged solution is obtained after about 100 iterations. The accuracy of the calculations for hydrostatic equilibrium is checked by the virial relation, i.e. the value of $|(2K + W + 3 \int P d^3 \mathbf{r})/W|$. Here K and W are the rotational energy and the gravitational energy, respectively. For typical models in this paper this value is around $\sim 10^{-3 \sim -4}$.

3. Initial models

Initial models are important to start investigating the effect of rotation on the stellar structures because the internal structures depend crucially on compositions of nuclei. However we cannot obtain the distributions of compositions from stellar evolution with rotation because there are no such codes. Therefore we will choose two initial models which have been constructed from calculations of spherical symmetric stars.

Two models are as follows:

1) Case A – 18 M_{\odot} star with an active hydrogen burning core. For computation of a spherical model we have used the evolution code developed by Saio et al. (1988). The initial model has been obtained by starting from a zero-age main-sequence (hereafter referred to as ZAMS) star with $X = 0.73$, $Y = 0.25$, $Z = 0.02$ and following evolution to the stage of 1.2×10^5 yr. The compositions in the central region where the CNO-network is included are listed in Table 1. The convective core reaches 7.56 M_{\odot} from the center.

2) Case B – Helium star of 5 M_{\odot} which has an active helium burning core. The evolution code developed by Nomoto & Hashimoto (1988) is used to obtain initial models. The initial model has been obtained also starting from a helium star with $X(^4\text{He}) = 0.9879$ and $X(^{14}\text{N}) = 0.0121$ and following evolution

Table 1. Mass fractions in the center of a $18 M_{\odot}$ star.

^1H	^4He	^{12}C	^{13}C	^{14}N	^{15}N	^{16}O	^{17}O
7.29(-1)	2.51(-1)	1.06(-4)	3.26(-5)	3.76(-3)	1.50(-7)	7.70(-3)	1.10(-4)

Table 2. Mass fractions in the center of a $5 M_{\odot}$ helium star.

^4He	^{12}C	^{16}O	^{20}Ne	^{24}Mg
6.64(-1)	2.90(-1)	2.81(-2)	1.32(-10)	9.06(-17)

to 2.9×10^6 yr after the stage of the gravitational contraction and that of helium ignition. The compositions in the central region included in the α -network are listed in Table 2. The convective core reaches $2.72 M_{\odot}$ from the center.

4. Results

We have computed equilibrium configurations for the rotation law (13). In Table 3 and Table 4, summarized are the results of selected models for nearly spherical stars and rotating stars. In Table 3, physical quantities for the sequences of $18 M_{\odot}$ star are shown. These stars are in the evolution stage just departing from the ZAMS stage and have hydrogen burning cores. In Table 4, given are the models of helium star of $5 M_{\odot}$ which have helium burning cores.

In these tables, the parameter B represents the degree of the concentration of the specific angular momentum in rotating stars. As mentioned before, the case $B = \infty$ means uniform rotation. The smaller the value of B becomes, the larger the angular velocity of the stellar core becomes. Physical quantities in these tables are: the mass M , the maximum temperature T_c , the maximum density ρ_c , the pressure at the maximum density P_c , the axis ratio of the polar radius R_p to the equatorial radius R_e , R_p/R_e , the luminosity L , the total angular momentum J , and the ratio of the rotational energy to the absolute value of the gravitational energy, $K/|W|$. It should be noted that the rotational configurations of $B = 2.0, 1.0, 0.5$ and 0.37 are those for critical rotational states (critical models), i.e. just before the state where the mass begins to shed from the equatorial surface. The results for nearly spherical stars agrees well with those obtained from the spherical symmetric code.

4.1. Common feature of rotating stars in burning stages

We will illustrate only the stellar structures for $18 M_{\odot}$ stars, because for the same parameter of B and the same ratio R_p/R_e , the general structure of the star is quite similar. In Figs. 1a–e shown are the density contours for $18 M_{\odot}$ stars where the differential rotation law is used. In Figs. 2a–c, the maximum temperature T_c , the maximum density ρ_c and the luminosity L in solar units are shown as a function of the total angular momentum. In Fig. 3, we show the luminosity versus $K/|W|$; this quantity can be regarded as the indicator of instability.

The ratio R_p/R_e is crucial to follow the equilibrium sequence up to the mass shedding. For $B = \infty$, we got the critical models when $R_p/R_e \sim 0.67$. Since the central temperature changes little, the maximum decrease in luminosity is 6.4% and 4.8% for Case A ($18 M_{\odot}$ star) and Case B ($5 M_{\odot}$ star), respectively. This result for Case A is consistent with computations of many authors who used the slow rotation approximation (Faulkner et al. 1968; Jackson 1970; Kippenhahn & Thomas 1970; Sackmann 1970; Sackmann & Anand 1970; Whelan et al. 1971; Papaloizou & Whelan 1973).

For $B = 2.0$, the density contour of the model at the stage of the mass shedding is almost the same as that for the uniform rotation as is shown in Fig. 1a. When $R_p/R_e \simeq 0.6$, mass shedding occurs as far as spheroidal configurations are concerned, i.e. if we do not consider “essentially” toroidal configurations for which the position of the maximum density is no more at the center but is located along the ring on the equator.

For $B \lesssim 1.0$, the luminosity drops more than 10% because the central temperature decreases as the deformation becomes significant. The decrease of the maximum temperature is due to the effect of the increase in the centrifugal force which makes the configuration flatter as shown in Fig. 1b. This tendency becomes remarkable for the model with $R_p/R_e = 0.3$ and $B = 0.5$ as seen in Fig. 1c, where we can see considerable polar flattening compared with the spherical configuration. As a consequence, the decrease of luminosity is 15% in Case A and 12% in Case B.

The luminosity depends on the shape of the deformed star as well as on the maximum temperature. In general the deformation seems to increase the luminosity, because the increase in the surface area which leads to more luminosity may overcome the effect of the centrifugal force which results in decrease of the temperature. However, for a deformed star with the same stellar mass, the luminosity decreases for all the present models. Thus we can consider the slight decrease of the central temperature is more effective than the effect of the shape change. This is because nuclear burning is very sensitive to the central temperature. Contrary to spheroidal stars, it should be noted that the luminosity of the toroidal object, which is similar to an accretion disk, increases due to the effect of the geometry (Hashimoto et al. 1993, 1995).

4.2. Considerably deformed H burning stars

For a particular parameter set, $R_p/R_e = 0.24$ and $B = 0.4$, we have a ‘core-envelope’ structure for the critical model; the star has not only a flat shape but has an extended envelope for $R/R_e \geq 0.5$ along the equator. The density contour and the density distribution along the equatorial plane are shown in Fig. 1d.

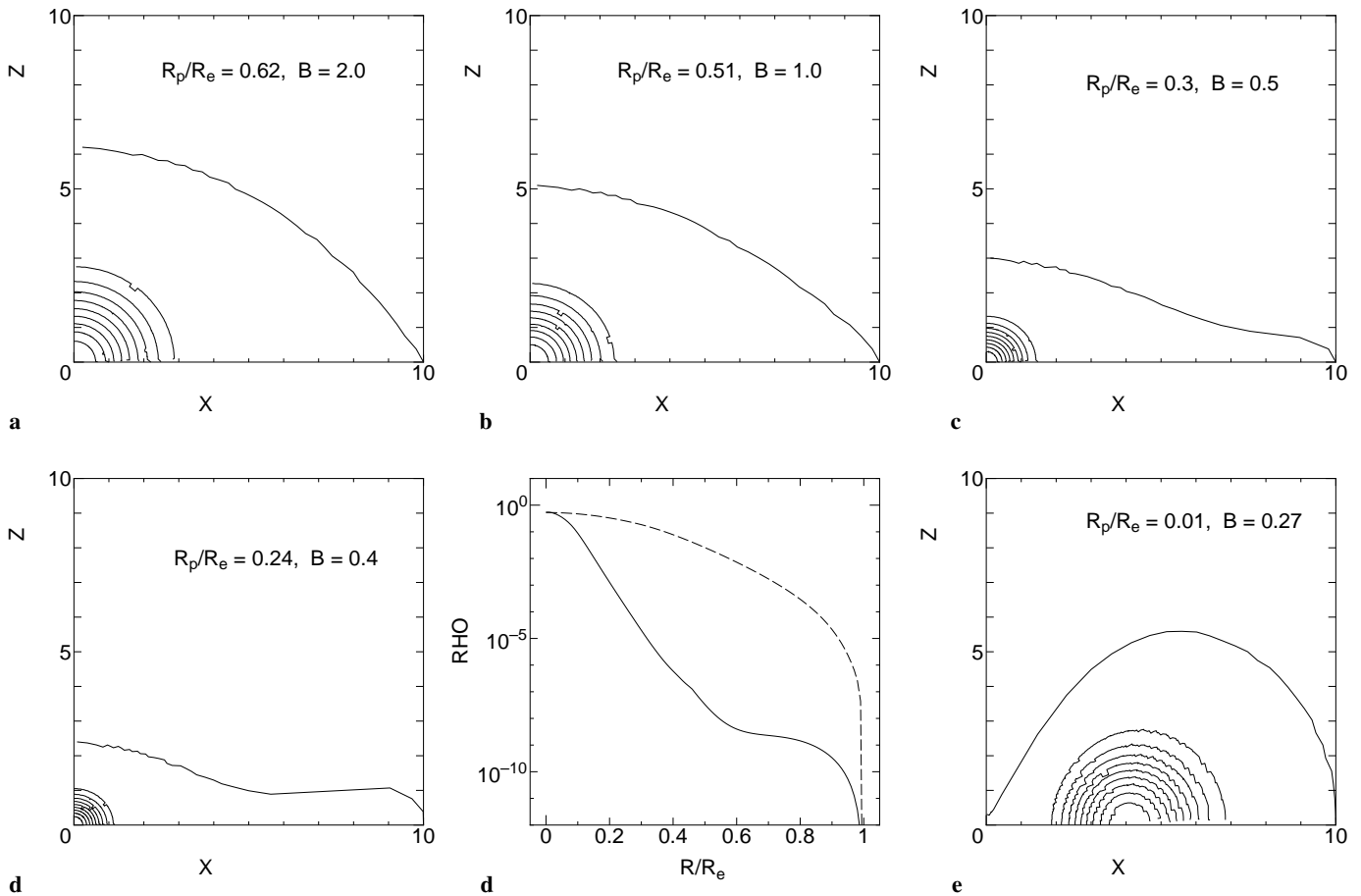


Fig. 1a–e. Contours of the constant density are shown for differentially rotating models. The density difference between two adjacent contours is 1/10 of the maximum density. **a** $R_p/R_e = 0.62$, $B = 2.0$. **b** $R_p/R_e = 0.51$, $B = 1.0$. **c** $R_p/R_e = 0.3$, $B = 0.5$. **d** $R_p/R_e = 0.24$, $B = 0.4$ (left figure). Density distribution versus R/R_e (right figure). Dashed line represents a spherical model. **e** $R_p/R_e = 0.01$, $B = 0.27$.

The radius is extended from $R_e = 5.31R_\odot$ in the spherical model to $R_e = 20.7R_\odot$ in the critical model. It should be noted that the appearance of the ‘envelope’ structure is due to rather delicate balance between the gravitational force and the centrifugal force.

Further increase in J causes a drastic change in the stellar configuration. If the angular momentum concentrates toward the inner core of the star, a toroid-like structure appears (Eriguchi & Müller 1985, Eriguchi & Müller 1991 and references quoted there); the maximum density locates at the off central point on the equator. To examine this extreme cases in realistic stars, we have performed the calculations of $B < 0.5$ for Case A. In the present study, a toroid-like structure has appeared for $B \leq 0.36$ before the model reaches a critical state. We show in Fig. 1e the density contour for $B = 0.27$ and $R_p/R_e = 0.01$. Since the central region rotates rapidly, the density around the center decreases drastically, and the maximum temperature at the off central point decreases down to $\approx 2.6 \times 10^7$ K. From Fig. 2a–c, we can see clearly significant changes in T_c , ρ_c , and L if $\log(J) > 53$. The significant decrease of the maximum temperature is possible because less pressure gradients are required to sustain the configuration due to the strong centrifugal force.

Although we have chosen a variety of the angular velocity or the angular momentum distributions for our models, the physical quantities seem to depend only on the global quantities which represent the amount of rotation such as the *total angular momentum* or the *ratio of the rotational energy to the gravitational energy*, as far as the mass of the star is fixed. This can be seen from Figs. 2 and 3 both for our models and for the results of Bodenheimer (1971). Therefore most of the rotational effect can be explained by specifying the total mass and the total angular momentum. In particular it is remarkable that the luminosity of stars with fixed masses seems to depend linearly on the ratio of the rotational energy to the gravitational energy as seen from Fig. 3, in spite of a large variety of the angular momentum distributions. In other words the luminosity of the rotating stars for a fixed mass can be expressed approximately by the following relation:

$$\log L = \log L_0 - \eta \frac{K}{|W|}, \quad (17)$$

where L_0 and η are the luminosity of the spherical star and a certain constant, respectively, and are given in Table 5.

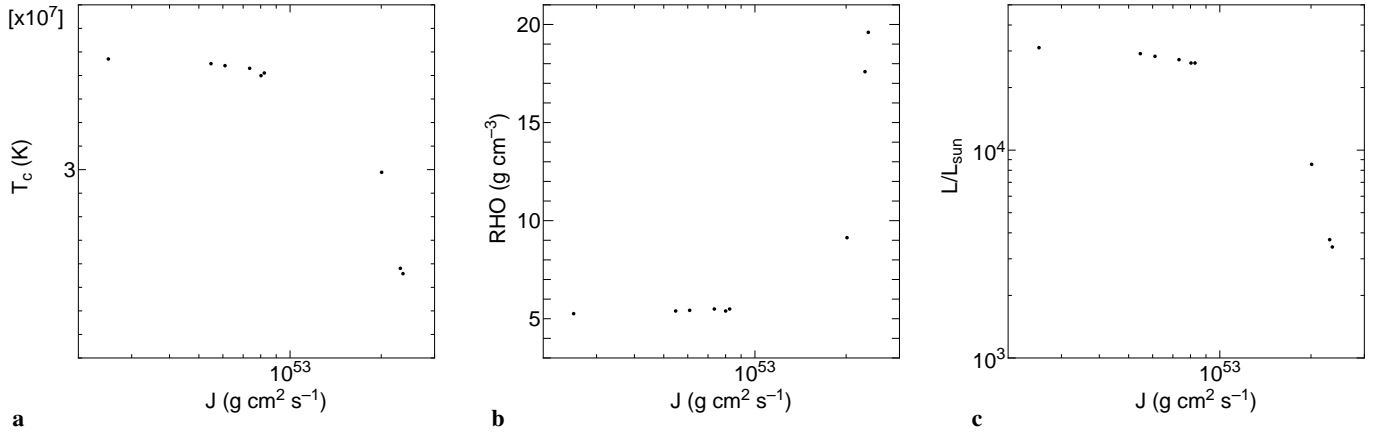


Fig. 2a–c. The maximum temperature **a**, the maximum density **b**, and the luminosity in solar units **c** are plotted as a function of the angular momentum $\log(J)$ for $18 M_{\odot}$ star model (Case A).

Table 3. Equilibrium models for $18 M_{\odot}$ with the assumed rotation laws. T_c , ρ_c , P_c and J are in units of K, g cm^{-3} , $\text{g cm}^{-1}\text{s}^{-2}$ and $10^{50} \text{g cm}^2 \text{s}^{-1}$, respectively. R_e , M , L are in solar units. P_c for $B = 0.27$ is the central value. * symbols denote that the model does not reach critical one.

B	M	T_c	ρ_c	P_c	R_p/R_e	R_e	L	J	$K/ W $
∞	18.03	3.47(7)	5.28(0)	2.88(16)	0.97	5.31	3.11(4)	2.52(2)	2.42(-3)
∞	18.04	3.45(7)	5.39(0)	2.91(16)	0.64	7.90	2.91(4)	5.48(2)	1.10(-2)
2.0	18.00	3.44(7)	5.43(0)	2.92(16)	0.62	8.06	2.83(4)	6.10(2)	1.35(-2)
1.0	18.04	3.43(7)	5.49(0)	2.94(16)	0.51	9.62	2.72(4)	7.34(2)	1.90(-2)
0.5	18.06	3.41(7)	5.49(0)	2.91(16)	0.30	16.4	2.63(4)	8.25(2)	2.34(-2)
0.37	18.02	3.40(7)	5.40(0)	2.85(16)	0.22	22.8	2.63(4)	8.02(2)	2.23(-2)
0.36*	18.06	2.99(7)	9.11(0)	3.94(16)	0.42	4.74	8.55(3)	2.01(3)	1.53(-1)
0.27*	18.03	2.56(7)	1.96(1)	1.04(2)	0.01	2.74	3.43(3)	2.36(3)	2.23(-1)

Table 4. Equilibrium models for helium star of $5 M_{\odot}$ with assumed rotation laws. T_c , ρ_c , P_c and J are in units of K, g cm^{-3} , $\text{g cm}^{-1}\text{s}^{-1}$ and $10^{50} \text{g cm}^2 \text{s}^{-1}$, respectively. R_e , M , L are in solar units.

B	M	T_c	ρ_c	P_c	R_p/R_e	R_e	L	J	$K/ W $
∞	5.00	1.80(8)	1.02(3)	1.32(19)	0.97	0.636	3.34(4)	1.21(1)	2.22(-3)
∞	5.02	1.79(8)	1.03(3)	1.32(19)	0.67	0.911	3.18(4)	2.63(1)	9.95(-3)
2.0	5.01	1.79(8)	1.04(3)	1.33(19)	0.62	0.977	3.11(4)	2.90(1)	1.21(-2)
1.0	5.00	1.78(8)	1.05(3)	1.33(19)	0.51	1.170	2.99(4)	3.45(1)	1.69(-2)
0.5	5.05	1.78(8)	1.04(3)	1.31(19)	0.30	2.012	2.95(4)	2.95(1)	2.05(-2)

As seen from Figs. 2a and c, the dependency of the maximum temperature and the luminosity on the angular momentum is quite similar. This can be clearly seen from Fig. 4 in which the luminosity is plotted against the maximum temperature. Thus the luminosity for rotating stars with a fixed mass can be expressed approximately as

$$\log L = \log L_1 + \lambda T_{7c} \quad (18)$$

where L_1 and λ are two constants whose values are also given in Table 5. Here T_7 is the temperature expressed in units of 10^7 K. Those constants appearing in formula (17) and (18) are obtained by using the least square fitting method. Values obtained by this fitting are tabulated in Table 5.

Table 5. Coefficients of the approximate formula (17) and (18).

burning stage	L_0	η	L_1	λ
H burning	3.273(4)	4.207	6.189	1.064
He burning	3.396(4)	3.077	0.892	0.2541

In Fig. 5 the maximum temperature is shown as a function of the maximum density. From this figure we can see clearly that the physical conditions for occurrence of nuclear burning are quite different from those for spherical stellar models. Moreover as far as the topology of configurations does not change, all models for fixed masses drop mostly on the straight line. This

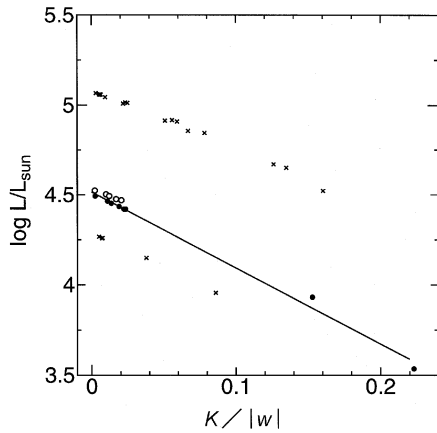


Fig. 3. The luminosity in solar units is shown as a function of the ratio of the kinetic energy to the gravitational energy $K/|W|$. The filled and open circles correspond to the $18 M_{\odot}$ star (Case A) and the $5 M_{\odot}$ star (Case B), respectively. Crosses denote models obtained by Bodenheimer (1971). The solid line represents the approximate formula (17) for the data of $18 M_{\odot}$ case.

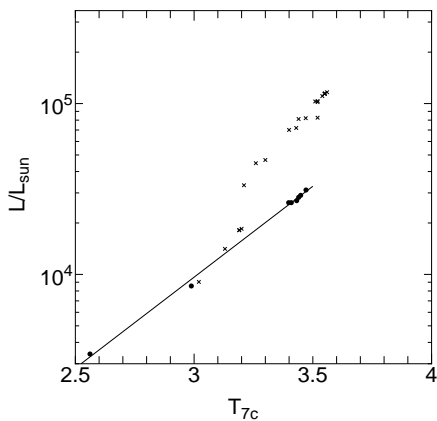


Fig. 4. The luminosity in solar units is shown as a function of the maximum temperature in units of 10^7 K for the $18 M_{\odot}$ star (filled circles: Case A). Crosses denote models obtained by Bodenheimer (1971). The solid line represents the approximate formula (18) for the data of $18 M_{\odot}$ case.

is the same tendency which was found by using the slow rotation approximation (Whelan et al. 1971). However, the topology change from spheroid to toroid may result in deviation from the straight lines on the $\log \rho_c$ – $\log T_c$ plane.

5. Discussions and concluding remarks

From the results in Tables 3 and 4, we can find strong dependence of the luminosity on the amount of the rotation. On the other hand, there are similar effects of rotation on the structure both for $18 M_{\odot}$ stars and for $5 M_{\odot}$ stars, despite large differences of the central temperature and the luminosity.

Generally, rotation causes to increase the stellar mass as far as the central temperature is kept fixed. On the contrary, if the stellar mass is kept fixed, as the stellar core rotates more

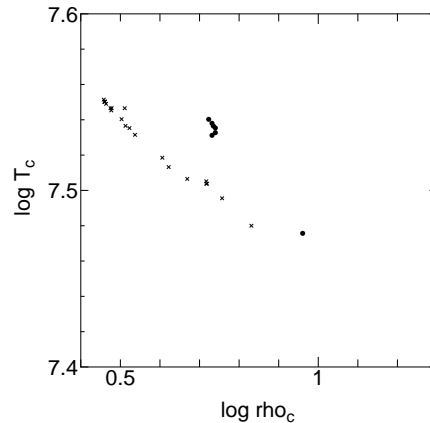


Fig. 5. The maximum temperature in units of 10^7 K is shown as a function of the maximum density for the $18 M_{\odot}$ star (filled circles: Case A). Crosses denote models obtained by Bodenheimer (1971).

and more rapidly, the maximum temperature is apt to decrease and the maximum density increases due to the effect of the centrifugal force as seen from Fig. 5. It should be noted that nuclear burning which is the source of the luminosity of the star is very sensitive to the temperature where the burning occurs. We can see from Fig. 3 and the relation (17) that the luminosity decreases as the ratio $K/|W|$ increases. For uniform rotation, the mass shedding occurs before the maximum temperature decreases appreciably because the equatorial velocity becomes large at the surface as the deformation becomes large. For differential rotation, the mass shedding does not occur and the maximum temperature decreases further compared with the case of uniform rotation as seen in Tables 3 and 4.

First, let us compare our results with those of Bodenheimer (1971). He has presented numerical results for homogeneous upper-main-sequence models of 15, 30, and $60 M_{\odot}$. The energy generation is assumed to be due to the CNO cycle running in equilibrium. Opacities are taken from Cox (1964) and the equation of state is that of an ideal gas plus radiation pressure. He has employed four different kinds of angular momentum distributions and concluded that difference of angular momentum distributions has only a negligible effect on the luminosity. This is consistent with our results where models with considerably different angular momentum distributions are computed.

On the other hand, increase in the total angular momentum J for a given stellar mass leads to large changes in the luminosity. In particular, the luminosity decreased by a factor of 5.6 for a $60 M_{\odot}$ with $\log J = 54.4$ compared with that of the spherical model. The central temperature decreased from 3.85×10^7 K to 3.29×10^7 K. Since our numerical treatment, physical inputs and initial models are very different from those of Bodenheimer, it is difficult to compare results quantitatively. Nevertheless, concerning uniform rotation, qualitatively our results agree well with his results; while the luminosity decrease is 5–7% in our case, it is 8% in his case. For differentially rotating case, as can be seen from Fig. 5 in his paper, a general trend of the behavior of ρ_c , T_c and L against J is consistent with our results which are shown in our Figs. 2a–c. Since we have computed significantly

deformed stars which he did not try to compute, the decrease in T_c , L and the increase in ρ_c for our models is much larger for $J > 2 \times 10^{53} \text{ g cm}^2 \text{ s}^{-1}$. It is not easy to compare our results with those of Clement (1979, 1994) because we could not get information about the values of the angular momentum of equilibrium states from his papers. However, qualitatively our results agree with those of Clement as far as models with $K|W| < 0.14$ are concerned.

As is well known, when the ratio $K/|W|$ becomes as large as 0.26, dynamical instability will set in (Bodenheimer & Ostriker 1973). Since the largest value of this ratio is 0.22 for the case of $B = 0.27$, our models will not suffer from dynamical instability of the bar mode. This is the case for Bodenheimer's models because the largest value of $K/|W|$ is 0.23 for $60 M_\odot$ star. As for the results of Clement (1979, 1994), since he could obtain only solutions with $K/|W| < 0.14$, all models are considered to be stable against the dynamical instability of bar mode. This stability argument and formula (17) give us that the lower limits of the luminosity for the $18M_\odot$ hydrogen burning stars and the $5M_\odot$ helium burning stars in stable states are $L_H \gtrsim 2.6 \times 10^3 L_\odot$ and $L_{He} \gtrsim 5.4 \times 10^3 L_\odot$, respectively. Similarly the lower limits of the maximum temperatures for stable hydrogen burning stars and stable helium burning stars are $T_c \gtrsim 2.5 \times 10^7 \text{ K}$ and $T_c \gtrsim 1.5 \times 10^8 \text{ K}$, respectively.

As seen from Table 3 and Fig. 2a, the maximum temperature drops significantly for $B < 0.37$. For these values of B we have not computed the complete sequence up to the model which suffers from mass shedding, if exist. Of course, for such a significantly differential rotation, there is a high possibility that the sequence will continue to toroidal configurations for which there appears a hole or a funnel near the rotation axis. It should be noted that for spheroidal configurations and toroidal configurations physical quantities do not always continue monotonically as seen from Figs. 4 and 5. This is due to the fact that toroidal configurations can be sustained by lower temperatures because of large centrifugal forces. Gaps of physical quantities between spheroidal models and toroidal models can be seen from Table 3 and Figs. 3, 4 and 5.

Contrary to the polytropic stars, the structure of the realistic star is very sensitive to the physical input, in particular to the nuclear reactions as can be expected. Consequently we may infer that stellar structures with active *burning shells* will be affected significantly due to rapid rotation. In fact, there remain two big problems which are reasonably considered to relate to stellar rotation; 1) why did the SN1987A explode as a blue supergiant (Saio et al. 1988)? 2) What was the cause of rings around of it (Eriguchi et al. 1992)? Furthermore the central condition of the star (the density, the temperature and the pressure) in an advanced stage of evolution will be influenced drastically by the differential rotation as inferred from Figs. 2a–c and Fig. 5.

As we have shown in the present investigation, we can obtain equilibrium structures of *realistic* rotating stars, i.e. time-independent solutions. It implies that if we can include further the entropy production due to gravitational contraction, we will be able to calculate quasi-static stellar evolutions of rotating stars. In this point our approach will lead to a new insight to the

pre-supernova models that have been studied only for spherical models (see e.g. a review by Hashimoto 1995). For example, an asymmetric explosion of supernova which should be related to the rotation of the core shows a very different feature compared with the spherical explosion: explosive nucleosynthesis products and the mass of the compact object are different from those of spherical computations (e.g. Nagataki et al. 1996).

Acknowledgements. We would like to thank the referee who pointed the papers of Clement to us. We would also like to express our gratitude to Dr. K. Arai for his comments. M.H. would like to thank Drs H. Yamaoka and H. Saio for discussions in making initial models. Numerical computations have been carried out at the computer centers of Kyushu University and of the University of Tokyo. M. H. is grateful to Drs. M. Arnould and M. Rayet for their hospitality at the Institut d'Astronomie et Astrophysique in Université Libre de Bruxelles. This work was supported in part by Grant-in-Aid for Scientific Research of the Ministry of Education, Science and Culture in Japan.

References

- Bodenheimer, P., 1971, ApJ 167, 153
- Bodenheimer, P., Ostriker, J.P., 1973, ApJ 180, 159
- Clayton, D.D., 1968, Principles of Stellar Evolution and Nucleosynthesis, (McGraw Hill, New York)
- Clement, M.J., 1974, ApJ 194, 709
- Clement, M.J., 1978, ApJ 222, 967
- Clement, M.J., 1979, ApJ 230, 230
- Clement, M.J., 1994, ApJ 420, 797
- Cox, A. N., 1964, unpublished
- Eriguchi, Y., Müller, E., 1985, A&A 146, 260
- Eriguchi, Y., Müller, E., Hachisu, I., 1986, A&A 168, 130
- Eriguchi, Y., Müller, E., 1991, A&A 248, 435
- Eriguchi, Y., Yamaoka, H., Nomoto, K., Hashimoto, M., 1992, ApJ 392, 243
- Eriguchi, Y., Müller, E., 1993, ApJ 416, 666
- Faulkner, J., Roxburgh, I.W., Strittmatter, P.A., 1968, ApJ 151, 203
- Hashimoto, M., Eriguchi, Y., Arai, K., Müller, E., 1993, A&A 268, 131
- Hashimoto, M., Eriguchi, Y., Müller, E., 1995, A&A 297, 135
- Hashimoto, M., 1995, Prog. Theor. Phys. 68, 795
- Iben, I. Jr., 1975, ApJ 196, 525
- Jackson, S., 1970, ApJ 160, 685
- Kippenhahn, R., Thomas, H.-C., 1970, in *IAU Colloq. 4, Stellar Rotation*, Ed. A. Slettebak, Reidel, p.20
- Kippenhahn, R., Weigert, A., 1990, *Stellar Structure and Evolution* (Springer, Heidelberg)
- Maeder, A., Meynet, G., 1987, A&A 182, 243
- Maeder, A., Meynet, G., 1988, A&A Suppl. 76, 411
- Müller, E., 1986, A&A 162, 103
- Nagataki, S., Hashimoto, M., Sato, K., Yamada, S., 1997 ApJ, in press
- Nomoto, K., Hashimoto, M., 1988, Phys. Rep. 163, 13
- Ostriker, J.P., Mark, J.W-K., 1968, ApJ 151, 1075
- Papaliolis, C., Karouska, M., Koechlin, L., Nisenson, P., Standley, C., Heathcote, S., 1989, Nature 338, 13
- Papaloizou, J.C.B., Whelan, J.A.J., 1973, MN 164, 1
- Pinsonneault, M.H., 1995, in *Stellar evolution: what should be done*, Proc. of the 32nd Liège Int. Astroph. Coll., Eds. A. Noels et al., p.65
- Penny, L. R., 1996, ApJ 463, 737
- Roxburgh, I.W., Griffith, J.S., Sweet, P.A., 1965, Z.f.Astro. 61, 203
- Sackmann, I.-J., 1970, A&A 8, 76

Sackmann, I.-J., Anand, S.P.S., 1970, ApJ 162, 105

Saio, H., Kato, M., Nomoto, K., 1988, ApJ 331, 388

Stellingwert, R.F., 1975, ApJ 195, 441

Tassoul, J.-L., 1978, Theory of Rotating Stars, Princeton University Press, Princeton

Trammell, R.S., Hines, C.D., Wheeler, C.J., 1993, ApJ 414, 21

Uryū, K., Eriguchi, Y., 1994, MN, 269, 24

Uryū, K., Eriguchi, Y., 1995, MN, 277, 1411

Whelan J.A.J., Papaloizou, J.C.B., Smith, R.C., 1971, MN 153, 9

This article was processed by the author using Springer-Verlag \TeX A&A macro package version 4.